Dynamical swinging between the insulating and metallic phases induced by the coherent amplitude mode excitation in 1T-TaS2

Qianhui Ren
　University of Tokyo

Takeshi Suzuki (✉ takeshi.suzuki@issp.u-tokyo.ac.jp)
　University of Tokyo

Teruto Kanai
　University of Tokyo

Jiro Itatani
　University of Tokyo

Shik Shin
　The University of Tokyo

Kozo Okazaki
　University of Tokyo

Article

Keywords:

Abstract

We investigate the nonequilibrium electronic structure of $1T$-TaS_2 by time- and angle-resolved photoemission spectroscopy. We observe that strong photo excitation induces the collapse of the Mott gap, leading to the photo-induced metallic phase. It is also found that the oscillation of photoemission intensity occurs as a result of the excitations of coherent phonons corresponding to the amplitude mode of the charge density wave (CDW). To study the dynamical change of the band dispersions modulated by the CDW amplitude mode, we perform analyses by using frequency-domain angle-resolved photoemission spectroscopy. We find that two different peak structures exhibit anti-phase oscillation with respect to each other. They are attributed to the minimum and maximum band positions in energy, where the single band is oscillating between them synchronizing with the CDW amplitude mode. We further find that the flat band constructed as a result of CDW band folding survives with the collapse of the Mott gap. Our results strongly suggest the CDW phase is more robust than the Mott insulating phase, and the lattice modulation corresponding to the CDW amplitude mode dynamically modulates the Mott gap.

Introduction

Transition-metal dichalcogenide (TMD) is a large class of widely studied layered two-dimensional materials. Many of TMDs show a metal-insulator transition (MIT) and some kind of an ordered ground state. Among them, $1T$-TaS_2 is a typical example and shows successive charge-density-wave (CDW) phase transitions [1] [2]. As temperature decreases, it undergoes incommensurate CDW (ICCDW), nearly-commensurate CDW (NCCDW), and commensurate CDW (CCDW) phases below 550, 350, and 180 K, respectively. In the CCDW phase, the 13 Ta atoms are modulated to form a Star of David cluster as schematically shown in Fig. 1(a). The band evolution around the G point revealed by angle-resolved photoemission spectroscopy is schematically shown in Figs. 1(b)-1(d) [3] [4] [5]. In the ICCDW phase, an electron band around the M point of the Brillouin-zone corner, which is derived from the Ta $5d$ orbital, crosses the Fermi level (E_F) near the G point. In the NCCDW phase, the band is folded to the G point due to the CDW potential and CDW hybridization gaps open at the band-crossing points due to the band folding. As a result, a flat band emerges around E_F, which can be regarded as evidence of the CDW band folding. Finally, in the CCDW phase, a band gap opens in the flat band, and this gap has been considered as a Mott gap [5].

Furthermore, $1T$-TaS_2 shows superconductivity by applying pressure [6] or chemical doping [7]. These intriguing features such as the coexistence of CDW and Mott-insulating phases or the emergence of superconductivity have motivated intensive studies of $1T$-TaS_2 for understanding the roles of electron-electron and electron-phonon interactions for a long time.

While many experimental methods have been employed to investigate physical properties in equilibrium conditions for $1T$-TaS_2 [4], ultrafast spectroscopies have provided an alternative route to investigate the nature underlying above phases via a non-equilibrium state [8]. Furthermore, strong photo-excitation can be found to alter this system to photo-induced metastable metallic phase at least just after pump, which

suggested the possibility of opto-electronic devices and triggered Fig. 2 (a) Fermi surface mapping for 1T-TaS$_2$ taken with a He discharge lamp at 240 K. The FS around the M point is indicated as a red oval. (b)-(i) Temperature-dependent ARPES images taken along the (b)-(e) G-M-G and (f)-(i) G-K-M directions. (j) Enlarged ARPES image corresponding to the area indicated as white box region in Fig. 2(i). intensive works [9] [10] [11]. Apart from the quest for such a hidden state, many ultrafast methods have been performed to investigate the interplays between electrons and phonons by perturbing or melting the charge order and analyzing the temporal response [12]. In this regard, time- and angle-resolved photoemission spectroscopy (TARPES) is a very powerful method because it can track the temporal band structure and gain direct information on nonequilibrium electronic states [13] [14] [15]. Especially in 1T-TaS$_2$, where the Fermi surface (FS) is located around the M point in the high temperature metallic phase, TARPES using the large photon energy obtained by high harmonic generation (HHG) using noble gas to reach the entire 1st Brillouin zone is very ideal [16] [17] [18] [19].

While many previous works using HHG TARPES successfully revealed the striking and fundamental electronic properties in 1T-TaS$_2$ including the initial melting dynamics of the Mott and CDW phases associated with the collapse of the Mott and CDW gaps [18], the band dispersions dynamically affected by the CDW amplitude mode, and their relations to the Mott and CDW phases are still missing. The reason might be lied in the difficulty to distinguish them in time-domain spectra. Recently we developed a new analysis method, which we call frequency-domain ARPES (FDARPES) [20]. This method allows us to distinguish the coexisting bands by selectively detecting band dispersions in the frequency-domain even during the photo-induced phase transition.

In this work, we applied TARPES and FDARPES methods to 1T-TaS$_2$ to investigate the dynamical properties of the Mott and CDW phases associated with the Mott gap and the flat band structure. We directly observe photo-induced melting of the Mott gap in the momentum space and the oscillating behavior as a result of the A$_{1g}$ coherent-phonon excitations in the TARPES image. Strikingly, further FDARPES analysis allows us to find out the flat band structure survives even during the photo-induced insulator-to-metal transition (IMT). Besides, the phase of FDARPES revealed the antiphase behavior between different two bands, which indicate the opposite sign of electron-phonon couplings between them.

Results And Discussion

In order to confirm the cleaved surfaces of the sample and temperature-induced phase transitions, we perform the static ARPES measurements. Figure 2(a) shows the Fermi surface (FS) mapping of 1T-TaS$_2$ measured at 240 K. The FS is clearly observed around the M point, which is indicated as a red oval. The photoemission intensity around the G point is ascribed to the flat band associated with the NCCDW phase [5]. Figures 2(b)-2(i) show the temperature-dependent ARPES images along the (b)-(e) G-M-G and (f)-(i) G-K-M directions. With decreasing temperature to 240 K, the flat band structure is more pronounced at the G point as a result of the band folding signifying the CDW phase [5]. With further decreasing

temperature to 140 K, a small gap of the flat band with respect to E_F is noticed, which corresponds to the Mott gap denoted as D_{Mott}[4]. Regarding the CDW phases, the ICCDW gap denoted as D_{ICCDW} around the M point increases with decreasing temperature. Besides, the two gaps associated with the CCDW phase denoted as $D_{CCDW1/2}$ are observed at the band dispersion around the G point. The Mott and CDW gaps are more clearly seen in the enlarged ARPES image shown in Fig. 2(j), which corresponds to the white-dashed box region indicated in Fig. 2(i). These findings are consistent with the previous report [4].

Now we discuss the TARPES results. Figure 3(a) shows the TARPES image before the arrival of the pump pulse around the G point along the M-G-M direction. While the flat band is clearly observed, the CCDW gap at the band crossing point due to the CDW folding is not so clear due to the lack of energy resolution, which is typical for the HHG TARPES measurements. Just after the strong pump pulse excitation of 4.2 mJ/cm^2, the system turns into the metallic phase [18]. Figure 3(b) shows the differential TARPES image at the delay time (Dt) of 240 fs. The increase and decrease of photoemission intensity are indicated as red and blue colors, respectively. It is noticed that the band dispersion crosses E_F as the red region around E_F increases. This demonstrates the photo-induced IMT with a collapse of the Mott gap as previously reported [18]. The complete set of TARPES images are shown in Fig. S1 [21] . The transient electron temperature at 160 fs is estimated to be higher than 600 K as shown in Fig. S2 [21], which is above the NCCDW transition temperature (350 K), above which the flat band disappears in equilibrium.

To study the dynamics in more detail, Fig. 3(c) shows the time-dependent photoemission intensity integrated at the energy-momentum region denoted as I and II in Figs. 3(a) and 3(b). Overall, the immediate increase (decrease) at Dt = 0 ps followed by the fast decrease (increase) and slow relaxation is observed for the region I (II). Besides, significant oscillations are confirmed to be superimposed onto both data. Moreover, these oscillations have anti-phase character with respect to each other. For highlighting the oscillatory components, we first subtract overall dynamics by fitting to a double-exponential function convoluted with a Gaussian, shown as the black solid lines in Fig. 3(c). Fourier transformations are performed for the subtracted data, and amplitudes for each frequency component are shown in Fig. 3(d). One can see the strong single peak at 2.5 THz, which corresponds to the breathing A_{1g} mode and is also called the CDW amplitude mode, confirmed by Raman spectroscopy [22], and the oscillation is as a result of coherent-phonon excitations based on the displacive excitation mechanism [23]. It should also be mentioned that the oscillation which appears in the TARPES measurements is due to the electron-phonon coupling, which connects the modulations between the lattice structure and electronic wave functions [24].

To further investigate the dynamical change of the electronic band dispersions modulated by the CDW amplitude mode, we proceed to FDARPES analysis. Figures 4(a) and 4(b) show the FDARPES images for amplitude and phase, respectively, at the frequency of 2.5 THz around the G point. FDARPES images at the different momentum cuts are shown in Fig. S3 [21]. One can notice that there exist two distinctive peak structures near and below E_F shown as black squares and circles, respectively, in Fig. 4(a). Interestingly, their phases shown in Fig. 4(b) are different by nearly p, which was already seen as an anti-

phase behavior in the time-dependent photoemission intensity in Fig. 3(c). This anti-phase character clearly shows that the single band oscillates between these two peak structures, synchronizing with the lattice modulation corresponding to the CDW amplitude mode, which is schematically shown in Fig. 5. The separation into the flat and M-shaped bands when the band shifts to the energetically lower position is due to the opening of the CDW gap, which is also seen at the temperature-dependent static ARPES shown in Fig. 2.

Strikingly, the shape of the band drastically changes between these two peak positions, and the flat band structure with a smaller Mott gap is clearly seen near E_F shown as black squares in Fig. 4. As seen in the temperature-dependent static ARPES shown in Fig. 2, the flat band structure is the signature of the CDW phase. Based on this connection, the observed flat band in the FDARPES spectra strongly suggests that the CDW band folding survives even though the Mott phase is strongly suppressed seen as a collapse of the Mott gap. Furthermore, it is unveiled that the CDW amplitude mode can dynamically modulate the Mott gap corresponding to the position of the band dispersions with respect to the E_F as well as the CDW gap corresponding to the distance between the flat and M-shaped band schematically seen in the blue circles in Fig. 5(b). These dynamical swinging between insulating and metallic phases related to the Mott and CDW phases are captured by FDARPES spectra. It is also of notice that these clear peaks are only elucidated in the frequency domain, never extracted in the time domain analysis as clearly noticed by seeing TARPES image in Fig. S2. The FDARPES technique relying on the lock-in amplification can greatly improve the signal-to-noise ratio by extracting only the relevant frequency component.

Conclusion

In summary, we have conducted TARPES measurements on $1T$-TaS$_2$ and proceeded to perform FDARPES analysis to understand the underlying nature of the photo-induced metallic phase. While the Mott-insulating gap is closed confirmed by TARPES, the flat band dispersion is clearly seen in the FDARPES image, which strongly indicates survival of the CDW band folding even during the photo-induced IMT. Our results shed new light in the electron-electron and electron-phonon interactions in this system.

Methods

Static angle-resolved photoemission spectroscopy

For the static ARPES, we used a photon energy of 21.2 eV obtained from a He discharge lamp (Scienta Omicron VUV 5050), and detected the photoelectrons using a Scienta R4000 analyzer.

Time- and angle-resolved photoemission spectroscopy

In the TARPES measurements, the experimental setup is similar to that of our previous reports [25] [26] but updated to the 10 kHz laser system(Spectra Physics, Solstice Ace) [27] [28]. The pules duration of the laser is 35 fs, the photon energy of the probe light is 21.7 eV corresponding to the 7th order high harmonic

generation, the total energy resolution is set to 250 meV, and the temporal resolution is evaluated to be ~70 fs. Details of the setup are described elsewhere [29]. All the spectra for the TARPES measurements are taken at the temperature of 15 K.

Sample

High-quality single crystals of $1T$-TaS_2 were provided by HG Graphene. Clean surfaces were obtained by cleaving *in situ*.

Declarations

Acknowledgements

Author contributions

Q. -H. R. and T. S. performed TARPES measurements and the data analysis. T. K. and J. I. conducted maintenance of HHG laser system and improvements of the TARPES apparatus. Q. -H. R., T. S. and K. O. wrote the manuscript. S. S. and K. O. designed the project. All the authors discussed the results and contributed to the manuscript.

Data availability

The data supporting the findings of this study are available from the corresponding author upon request.

Competing interests

The authors declare no competing interests.

References

1. J. A. Wilson, F. J. Di Salvo, and S. Mahajan, "Charge-density waves and superlattices in the metallic layered transition metal dichalcogenides," *Adv. Phys.* **24**, 195 (1975).
2. P. Fazekas and E. Tosatti, "Electrical, structural and magnetic properties of pure and doped $1T$-TaS2," *Philos. Mag. B* **39**, 229 (1979).
3. F. Clerc, C. Battaglia, M. Bovet, L. Despont, C. Monney, H. Cercellier, M. G. Garnier, P. Aebi, H. Berger, and L. Forró, "Lattice-distortion-enhanced electron-phonon coupling and Fermi surface nesting in $1T$-

TaS$_2$," *Phys. Rev. B* **74**, 155114 (2006).

4. I. Lutsyk, M. Rogala, P. Dabrowski, P. Krukowski, P. J. Kowalczyk, A. Busiakiewicz, D. A. Kowalczyk, E. Lacinska, J. Binder, N. Olszowska, M. Kopciuszynski, K. Szalowski, M. Gmitra, R. Stepniewski, M. Jalochowski, J. J. Kolodziej, A. Wysmolek, and Z. Klusek, "Electronic structure of commensurate, nearly commensurate, and incommensurate phases of 1T-TaS$_2$ by angle-resolved photoelectron spectroscopy, scanning tunneling spectroscopy, and density functional theory," *Phys. Rev. B* **98**, 195425, (2018).

5. Y. D. Wang, W. L. Yao, Z. M. Xin, T. T. Han, Z. G. Wang, L. Chen, C. Cai, Y. Li, and Y. Zhang, "Band insulator to Mott insulator transition in 1T-TaS$_2$," *Nat. Commun.* **11**, 4215 (2020).

6. B. Sipos, A. F. Kusmartseva, A. Akrap, H. Berger, L. Forró, and E. Tutiš, "From Mott state to superconductivity in 1T-TaS$_2$", *Nat. Mater.* **7**, 960 (2008).

7. Y. Liu, R. Ang, W. J. Lu, W. H. Song, L. J. Li , Y. P. Sun, "Superconductivity induced by Se-doping in layered charge-density-wave system 1T-TaS$_{2-x}$Se$_x$", *Appl. Phys. Lett.* **102**, 192602 (2013).

8. J. Demsar, L. Forró, H. Berger, and D. Mihailovic, "Femtosecond snapshots of gap-forming charge-density-wave correlations in quasi-two-dimensional dichalcogenides 1T-TaS$_2$ and 2H-TaSe$_2$", *Phys. Rev. B* **66**, 041101, (2002).

9. L. Stojchevska, I. Vaskivskyi, T. Mertelj, P. Kusar, D. Svetin, S. Brazovskii, and D. Mihailovic, "Ultrafast Switching to a Stable Hidden Quantum State in an Electronic Crystal", *Science* **344**, 177 (2014).

10. V. Igor, G. Jan, B. Serguei, S. Damjan, S. Petra, G. Evgeny, A. Mihailovic Ian, M. Tomaz, and M. Dragan, "Controlling the metal-to-insulator relaxation of the metastable hidden quantum state in 1T-TaS$_2$", *Sci. Adv.* **1**, e1500168 (2015).

11. Q. Stahl, M. Kusch, F. Heinsch, G. Garbarino, N. Kretzschmar, K. Hanff, K. Rossnagel, J. Geck, and T. Ritschel, "Collapse of layer dimerization in the photo-induced hidden state of 1T-TaS$_2$", *Nat. Commun.* **11**, 1247 (2020).

12. M. Eichberger, H. Schäfer, M. Krumova, M. Beyer, J. Demsar, H. Berger, G. Moriena, G. Sciaini, and R. J. D. Miller, "Snapshots of cooperative atomic motions in the optical suppression of charge density waves", *Nature* **468**, 799 (2010).

13. L. Perfetti, P. A. Loukakos, M. Lisowski, U. Bovensiepen, H. Berger, S. Biermann, P. S. Cornaglia, A. Georges, and M. Wolf, "Time Evolution of the Electronic Structure of 1T-TaS$_2$ through the Insulator-Metal Transition", *Phys. Rev. Lett.* **97**, 067402 (2006).

14. M. Ligges, I. Avigo, D. Golež, H. U. R. Strand, Y. Beyazit, K. Hanff, F. Diekmann, L. Stojchevska, M. Kalläne, P. Zhou, K. Rossnagel, M. Eckstein, P. Werner , and U. Bovensiepen, "Ultrafast Doublon Dynamics in Photoexcited 1T-TaS$_2$", *Phys. Rev. Lett.* **120**,166401 (2018).

15. I. Avigo, F. Queisser, P. Zhou, M. Ligges, K. Rossnagel, R. Schützhold, and U. Bovensiepen, "Doublon bottleneck in the ultrafast relaxation dynamics of hot electrons in 1T-TaS$_2$", *Phys. Rev. Res.* **2**, 022046 (2020).

16. K. Ishizaka, T. Kiss, T. Yamamoto, Y. Ishida, T. Saitoh, M. Matsunami, R. Eguchi, T. Ohtsuki, A. Kosuge, T. Kanai, M. Nohara, H. Takagi, S. Watanabe, and S. Shin, "Femtosecond core-level photoemision spectroscopy on 1T-TaS using a 60-eV laser source," *Phys. Rev. B* **83**, 081104(R) (2011).

17. J. C. Petersen, S. Kaiser, N. Dean, A. Simoncig, H. Y. Liu, A. L. Cavalieri, C. Cacho, I. C. E. Turcu, E. Springate, F. Frassetto, L. Poletto, S. S. Dhesi, H. Berger, and A. Cavalleri, "Clocking the Melting Transition of Charge and Lattice Order in 1T-TaS$_2$ with Ultrafast Extreme-Ultraviolet Angle-Resolved Photoemission Spectroscopy", *Phys. Rev. Lett.* **107**, 177402 (2011).

18. S. Hellmann, T. Rohwer, M. Kalläne, K. Hanff, C. Sohrt, A. Stange, A. Carr, M. M. Murnane, H. C. Kapteyn, L. Kipp, M. Bauer, and K. Rossnagel, "Time-domain classification of charge-density-wave insulators," *Nat. Commun.* **3**, 1069 (2012).

19. A. Simoncig, M. Stupar, B. Ressel, T. Saha, P. Rebernik Ribic , G. De Ninno, "Dissecting Mott and charge-density wave dynamics in the photoinduced phase of 1T-TaS$_2$", *Phys. Rev. B* **103**, 155120 (2021).

20. T. Suzuki, Y. Shinohara, Y. Lu, M. Watanabe, J. Xu, K. L. Ishikawa, H. Takagi, M. Nohara, N. Katayama, H. Sawa, M. Fujisawa, T. Kanai, J. Itatani, T. Mizokawa, S. Shin, and K. Okazaki, "Detecting electron-phonon coupling during photoinduced phase transition", *Phys. Rev. B* **103**, L121105 (2021).

21. See Supplemental Material at URL for time- and angle-resolved photoemission images at the G point, estimation of the electron temperatures before, and after photo-excitations and FDARPES images at the different momentum cuts.

22. J. R. Duffey, R. D. Kirby, and R. V. Coleman, "Raman scattering from 1T-TaS$_2$", *Solid State Commun.* **20**, 617 (1976).

23. H. J. Zeiger, J. Vidal, T. K. Cheng, E. P. Ippen, G. Dresselhaus, and M. S. Dresselhaus, "Theory for displacive excitation of coherent phonons", *Phys. Rev. B* **45**, 768 (1992).

24. U. De Giovannini, H. Hübener, S. A. Sato, and A. Rubio, "Direct Measurement of Electron-Phonon Coupling with Time-Resolved ARPES", *Phys. Rev. Lett.* **125**, 136401 (2020).

25. K. Okazaki, Y. Ogawa, T. Suzuki, T. Yamamoto, T. Someya, S. Michimae, M. Watanabe, Y. Lu, M. Nohara, H. Takagi, N. Katayama, H. Sawa, M. Fujisawa, T. Kanai, N. Ishii, J. Itatani, T. Mizokawa, S. Shin, "Photo-induced semimetallic states realised in electron-hole coupled insulators", *Nature Commun.* **9**, 4322 (2018).

26. M. Watanabe, T. Suzuki, T. Someya, Y. Ogawa, S. Michimae, M. Fujisawa, T. Kanai, J. Itatani, T. Saitoh, S. Shin, K. Okazaki, "Photo-Excitation Band-Structure Engineering of 2H-NbSe2 Probed by Time- and Angle-Resolved Photoemission Spectroscopy", *J. Phys. Soc. Jpn.* **91**, 064703 (2022).

27. T. Suzuki, T. Iimori, S. J. Ahn, Y. Zhao, M. Watanabe, J. Xu, M. Fujisawa, T. Kanai, N. Ishii, J. Itatani, K. Suwa, H. Fukidome, S. Tanaka, J. R. Ahn, K. Okazaki, S. Shin, F. Komori, I. Matsuda, "Ultrafast Unbalanced Electron Distributions in Quasicrystalline 30° Twisted Bilayer Graphene", *ACS Nano* **13**, 11981 (2019).

28. Y. Zhao, T. Suzuki, T. Iimori, H.-W. Kim, J. R. Ahn, M. Horio, Y. Sato, Y. Fukaya, T. Kanai, K. Okazaki, S. Shin, S. Tanaka, F. Komori, H. Fukidome, I. Matsuda, *Phys. Rev. B* **105**, 115304 (2022).

29. T. Suzuki, S. Shin, and K. Okazaki, "HHG-laser-based time- and angle-resolved photoemission spectroscopy of quantum materials," *J. Electron Spectrosc. Relat. Phenom.* **251**, 147105 (2021).
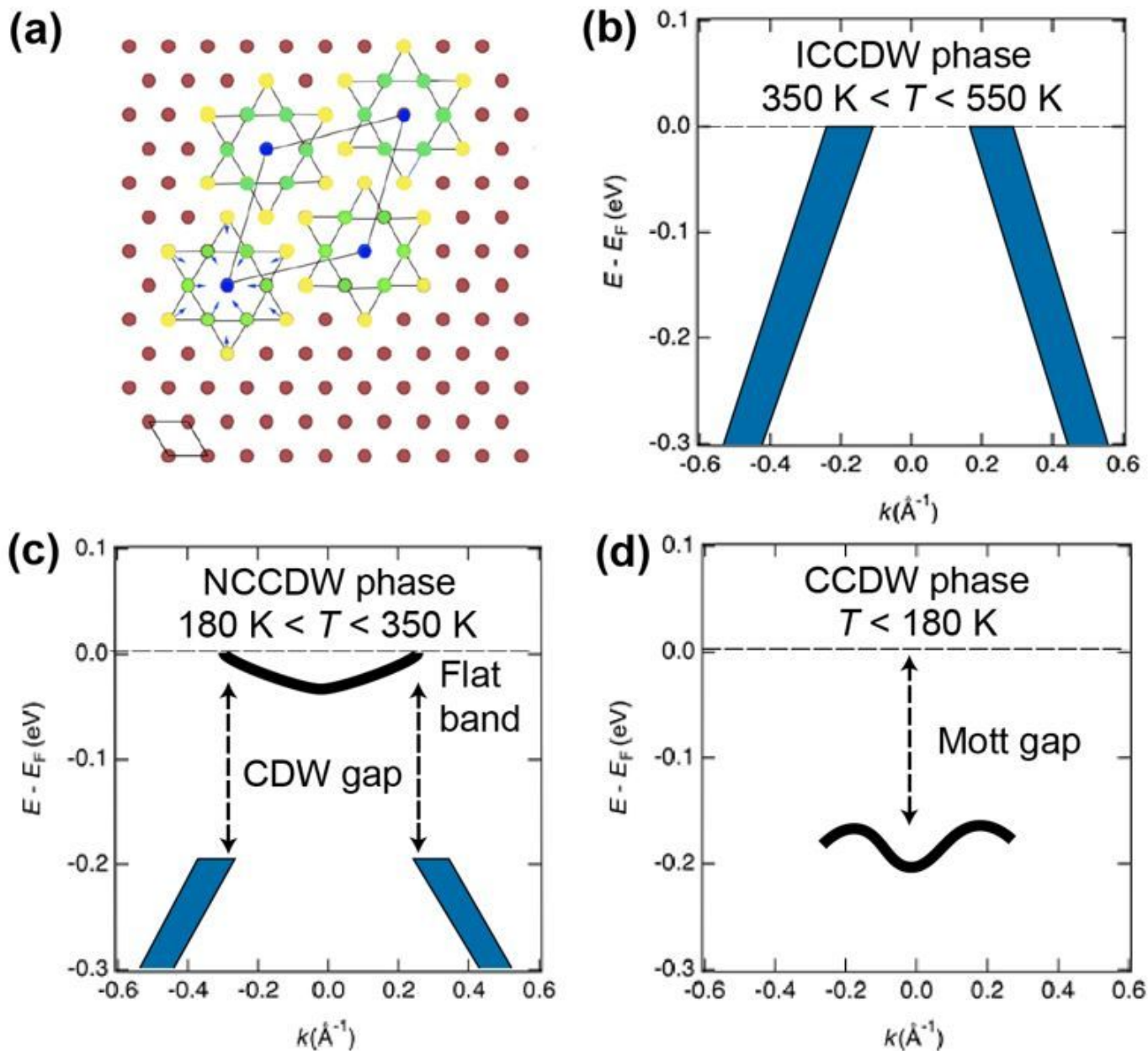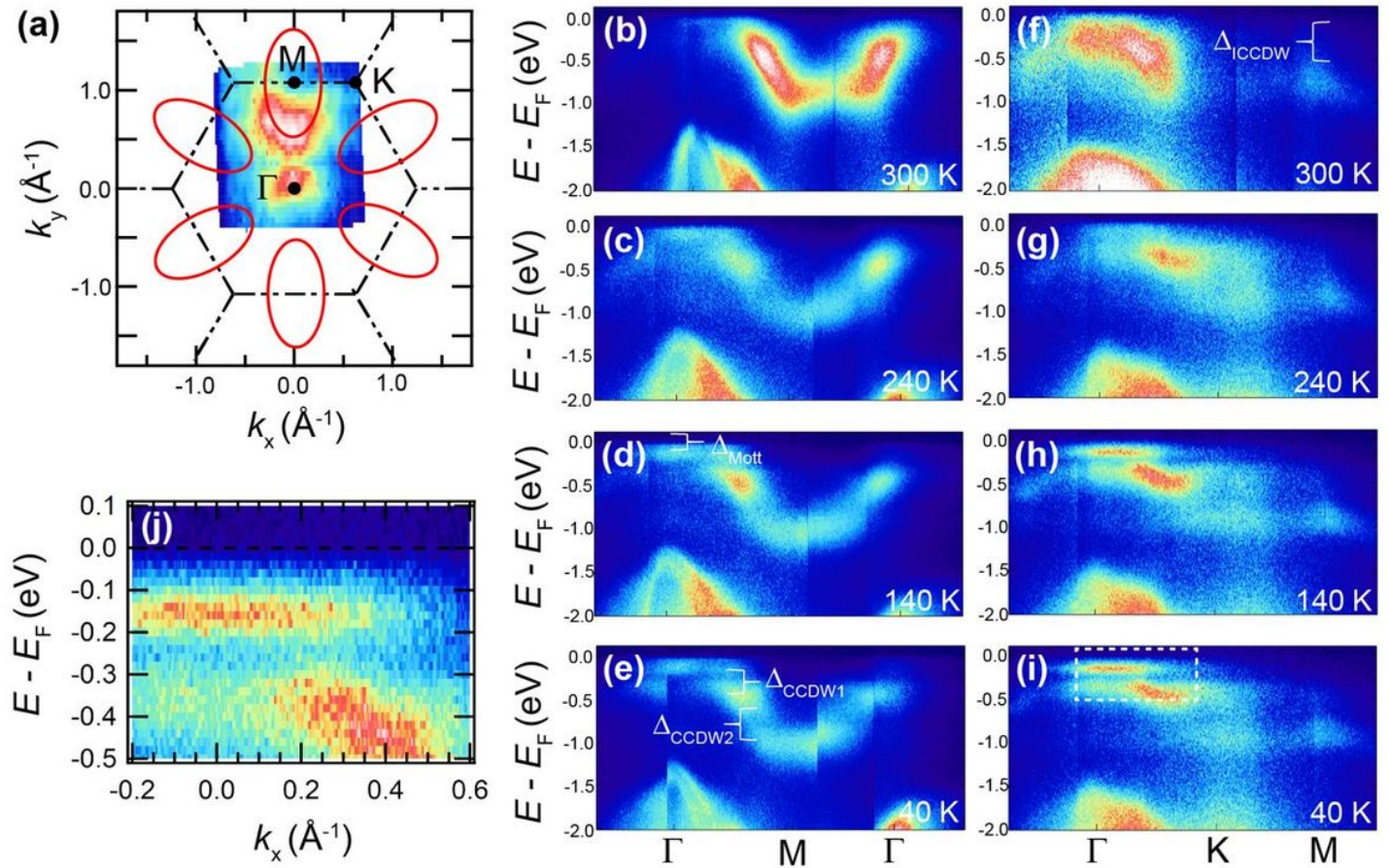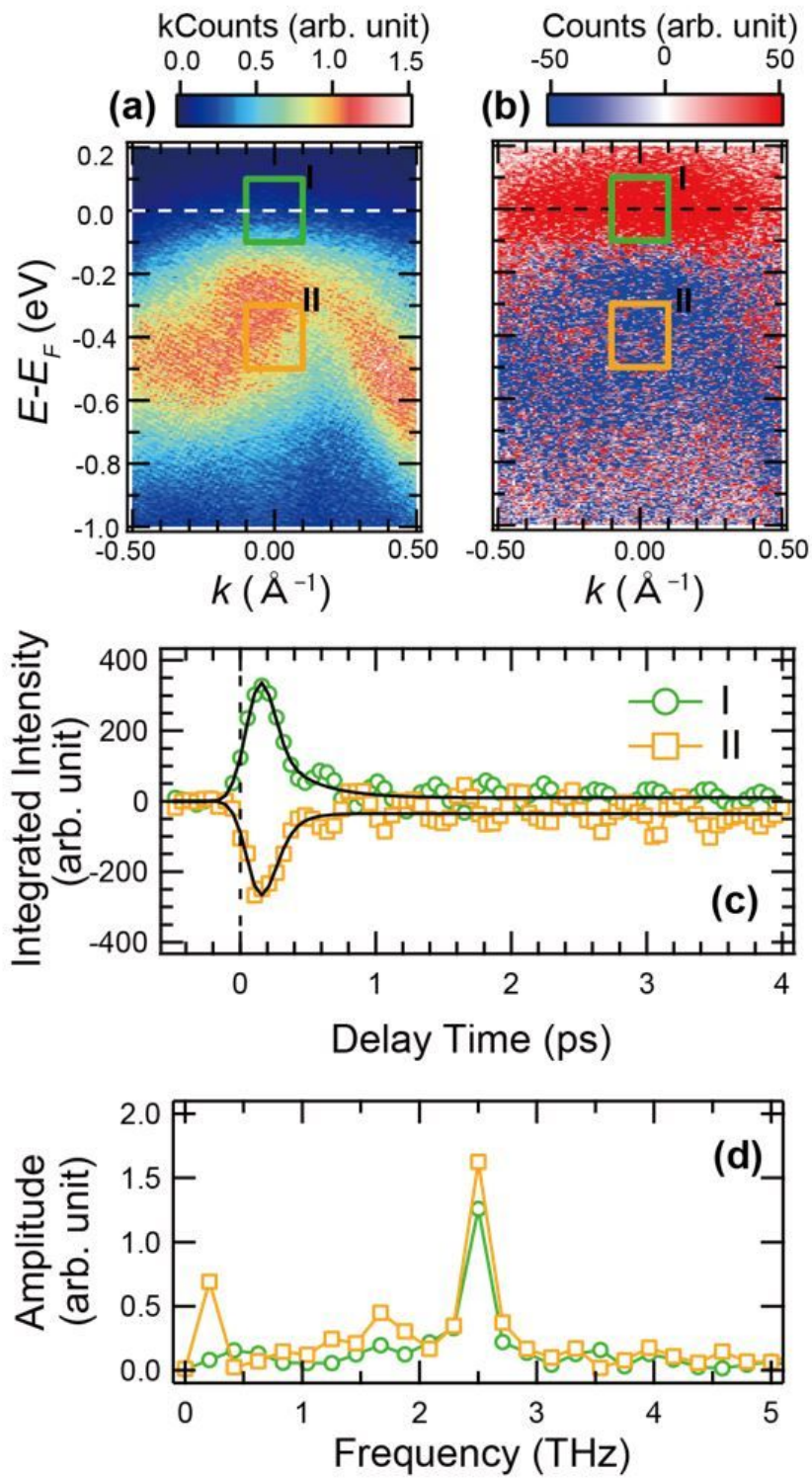
Figures

Figure 1

(a) Schematic illustration for the in-plane lattice modulations in the commensurate CDW phase (CCDW).
(b)-(d) Schematic illustration of the band evolution crossing the different phases [5].
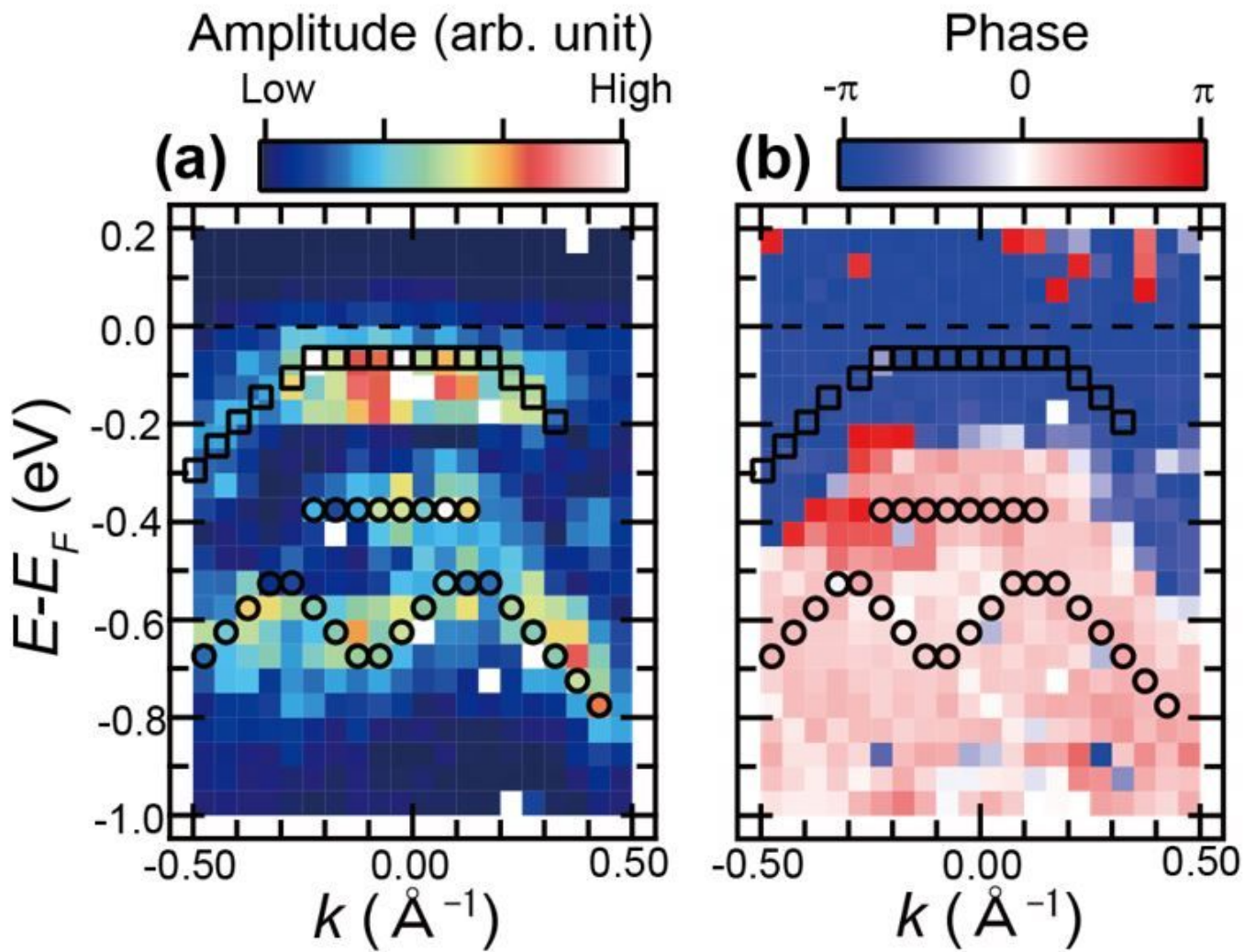
Figure 2

(a) Fermi surface mapping for 1T-TaS$_2$ taken with a He discharge lamp at 240 K. The FS around the M point is indicated as a red oval. (b)-(i) Temperature-dependent ARPES images taken along the (b)-(e) G-M-G and (f)-(i) G-K-M directions. (j) Enlarged ARPES image corresponding to the area indicated as white box region in Fig. 2(i).
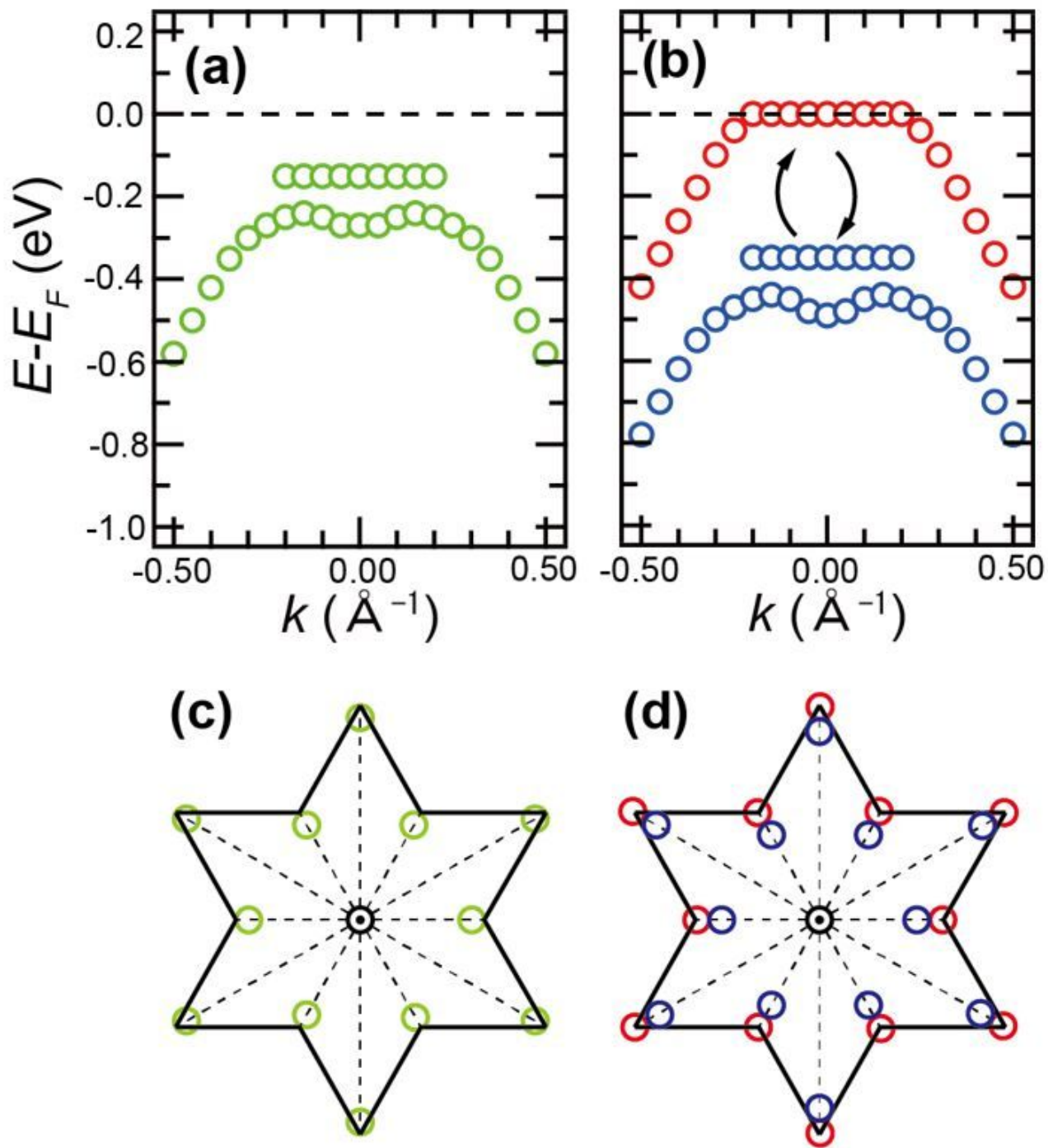
Figure 3

Frequency-domain ARPES images for (a) amplitude and (b) phase at the frequency of 2.5 THz. Black markers show the peak positions for the amplitude (a).

Figure 4

Frequency-domain ARPES images for (a) amplitude and (b) phase at the frequency of 2.5 THz. Black markers show the peak positions for the amplitude (a).

Figure 5

Schematic illustration of the band dispersions at the (a) equilibrium and (b) after photoexcitation. Schematic illustration of the displacement of Ta atoms at the (c) equilibrium and (d) after photoexcitation. Red and blue markers in the band dispersions shown in (b) corresponds to the displacement of Ta atoms shown as red and blue markers in (d).

Supplementary Files

This is a list of supplementary files associated with this preprint. Click to download.

- TaS2NinSMfin.docx